Resonance Energy Transfer from β-Cyclodextrin-Capped ZnO:MgO Nanocrystals to Included Nile Red Guest Molecules in Aqueous Media

Sabyasachi Rakshit and Sukumaran Vasudevan*

Department of Inorganic and Physical Chemistry, Indian Institute of Science, Bangalore-560012, India

ABSTRACT Core—shell ZnO:MgO nanocrystals have been synthesized by a sequential preparative procedure and capped with carboxymethyl β-cyclodextrin (CMCD) cavities, thereby rendering the surface of the nanocrystals hydrophilic and the particles water-soluble. The water-soluble CMCD-capped ZnO:MgO nanocrystals emit strongly in the visible region (450—680 nm) on excitation by UV radiation and are stable over extended periods and over a range of pH values. The integrity of the cyclodextrin cavities is preserved on capping and retains their capability for complexation of hydrophobic species in aqueous solutions. Here we report the use of the water-soluble cyclodextrin-capped ZnO:MgO nanocrystals as energy donors for fluorescence resonance energy transfer studies. The organic dye Nile Red has been included within the anchored cyclodextrin cavities to form a noncovalent CMCD ZnO:MgO—Nile Red assembly in aqueous solution. Significant Nile Red fluorescence at 640 nm is observed on band gap excitation of the ZnO:MgO in the UV, indicating efficient resonance energy transfer (RET) from the nanocrystals to the included dye. The number of acceptor molecules interacting with a single donor in the CMCD ZnO:MgO—Nile Red assembly may be altered by controlling the filling up of the anchored cavities by Nile Red, leading to a variation in the efficiency of resonance energy transfer. The donor—acceptor distance was estimated from the efficiency measurements. The Nile Red emission following RET shows a pronounced thermochromic shift, suggesting the possible use of the CMCD ZnO:MgO—Nile Red assembly as thermometers in aqueous solutions.

KEYWORDS: water-soluble ZnO:MgO nanocrystals · carboxymethyl β-cyclodextrin-capped · trap-state emission · resonance energy transfer · Nile Red

Semiconductor nanocrystals with size-tunable photoluminescence are promising alternatives to organic dyes for fluorescence-based applications.[1,2] II—VI semiconductors based on cadmium chalcogenides are the front-runners for such applications because of their intense absorption, high quantum yield, and, more importantly, luminescence properties that are size-dependent and hence tunable over a wide wavelength range.[3] They are also excellent donors in fluorescence resonance energy transfer (FRET)-based applications due to their narrow emission and broad excitation spectra, enabling the effective separation of the donor and acceptor fluorescence.[4] Studies of FRET between different colored II—VI semiconductor nanocrystals[5] and from the nanocrystals to dye-labeled polymers[6] and biomolecules[7–11] including DNA[12] have been reported. FRET-based detection and assay of analytes in water have become increasingly important.[13] Such applications require that the nanocrystals be water-soluble, and consequently, a number of innovative methods have been developed to render II—VI semiconductor nanocrystals water-soluble.[14] Their superior optical properties are, however, offset by the fact that the Cd, Se, and, to a lesser extent, S are toxic and pose a potential pollution hazard.[15] This has been recognized and has led to efforts to develop emissive nanocrystals that do not involve these elements.[16]

ZnO is a well-known II—IV semiconductor with a band gap of 3.2 eV that exhibits an efficient blue-green emission with high efficiency that has been attributed to deep trap states lying midway between the conduction and valence bands.[17] Nanoparticles of ZnO have been studied for use as photocatalysts, sensors, and phosphors.[18] The emission spectra of ZnO have been extensively studied; the as-prepared ZnO nanocrystals exhibit a sharp UV excitonic emission at ~380 nm (3.3 eV) and a broad intense visible emission at ~550 nm (2.2 eV). The ratio of the intensities of the visible trap emission to the UV excitonic emission is strongly dependent on particle size being larger the smaller the nanocrystal; for ZnO nanocrystals larger than 12 nm, the visible emission is usually absent.[19] In principle, visible light emitting ZnO nanocrystals would be ideal candidates as replacement for Cd-based fluorescent labels since they are nontoxic, less expensive, and chemically stable in air. However, the nanoscale ZnO tend to aggregate

*Address correspondence to svipc@ipc.iisc.ernet.in.

Received for review March 13, 2008 and accepted June 17, 2008.

Published online July 1, 2008.
10.1021/nn800152a CCC: $40.75

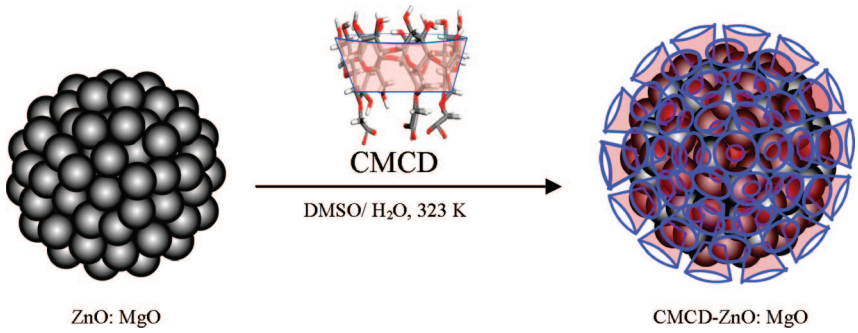

Scheme 1.

or undergo Ostwald ripening because of high surface free energy, resulting in the disappearance of the visible emission. Attempts to stabilize the ZnO nanocrystals in solvent dispersions by capping have usually resulted in the quenching of the visible trap emission.[20] It has been shown that small additions of Mg (<10%) resulting in the surface segregation of MgO on ZnO nanocrystals prevented the aggregation of the nanoparticles and formation of nonradiative recombination sites, resulting in a more intense and stable green photoluminescence.[21] The visible emission involves deep trap states arising from oxygen vacancies and also either electrons and/or holes in shallow trap states that originate from surface species/states in these large surface to bulk volume nanocrystals.[22,23]

Here we describe a simple procedure to obtain water-soluble ZnO:MgO nanocrystals that are stable over a range of pH values and which fluoresce in the visible. Water solubility is achieved by capping the ZnO:MgO nanocrystals with carboxymethyl β-cyclodextrin (CMCD) cavities. The anionic derivative of β-cyclodextrin, CMCD, is formed by substitution of part of the primary hydroxyl groups located at the narrower rim of the cyclodextrin toroidal cavity by carboxymethyl groups. These groups can coordinate to the metal oxide surface in much the same way as carboxylic groups of fatty acids. Capping of nanocrystals by cyclodextrin cavities are known to render the surface hydrophilic due to the existence of hydroxyl groups on the rim of the cyclodextrin cavity.[24] A unique features of the CMCD-capped ZnO:MgO nanocrystals is that the surface-anchored cyclodextrin cavities retain their host capabilities for inclusion of small hydrophobic molecules. Here we show how the fluorescence properties of the water-soluble CMCD ZnO:MgO nanocrystals can be modified by inclusion of the hydrophobic organic dye, Nile Red, within the anchored cavities. We are able to demonstrate that FRET occurs from the visible light emitting ZnO:MgO nanocrystals to Nile Red in the noncovalent supramolecular CMCD ZnO:MgO−Nile Red assembly.

RESULTS AND DISCUSSION

ZnO:MgO nanocrystals were synthesized by a sequential preparative procedure that involved formation of the ZnO core followed by the MgO shell. Cyclodextrin capping of the ZnO:MgO nanocrystals was achieved by simple mass exchange, addition of CMCD, with an average degree of carboxymethyl substitutions of 3.8 per cyclodextrin molecule, to the ZnO:MgO nanocrystals resuspended in 10% H_2O/DMSO (Scheme 1).

Representative X-ray diffraction patterns and TEM images of the cyclodextrin-capped ZnO:MgO powders are shown in Figure 1. For comparison, the X-ray diffraction pattern of cyclodextrin-capped ZnO nanocrystals without Mg is also shown. Both patterns (Figure 1a) are consistent with the hexagonal phase of ZnO, a conclusion supported by high-resolution TEM (inset of Figure 1b), which show lattice fringes with a spacing of 2.6 Å characteristic of the 002 planes of wurtzite. The particle size calculated from the Debye−Scherrer broadening is 6 nm. It is well-known that core/shell II−IV semiconductor nanocrystals such as CdS:Mn/ZnS and CdS/CdSe exhibit no X-ray broadening upon deposition of the shell layer.[25] Similarly, the MgO shell is not expected to affect the XRD peak width of the ZnO core, implying that the size of 6 nm corresponds to the ZnO core in ZnO:MgO nanocrystals. Particle sizes were obtained by analyzing >100 nanocrystals from the TEM image (Figure 1b). The average particle size was 6.4 (±1.5) nm, consistent with the values from X-ray broadening. Infrared and Raman spectroscopy of the ZnO:MgO nanocrystal powders clearly establish the presence of CMCD cavities coordinated to the metal oxide surface (see Supporting Information). The molar ratio of CMCD per

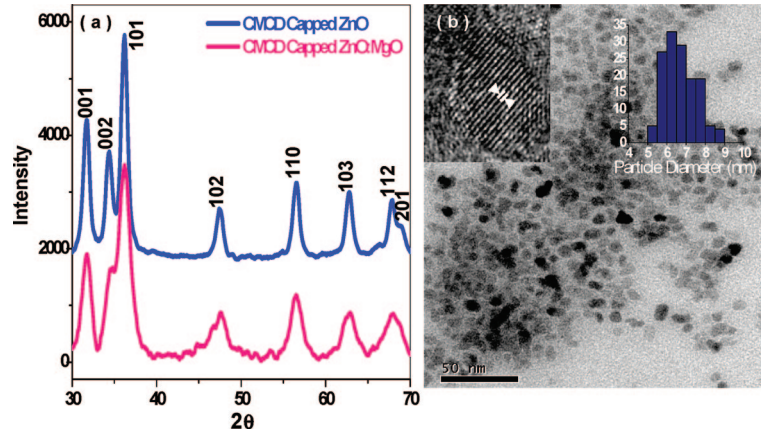

Figure 1. (a) Powder XRD patterns for the CMCD-capped ZnO:MgO and ZnO. (b) TEM images of the CMCD-capped ZnO:MgO. The inset on the left shows a high-resolution image showing lattice fringes with a spacing of 2.6 A. The histogram of particle sizes in the TEM image is shown in the right inset.

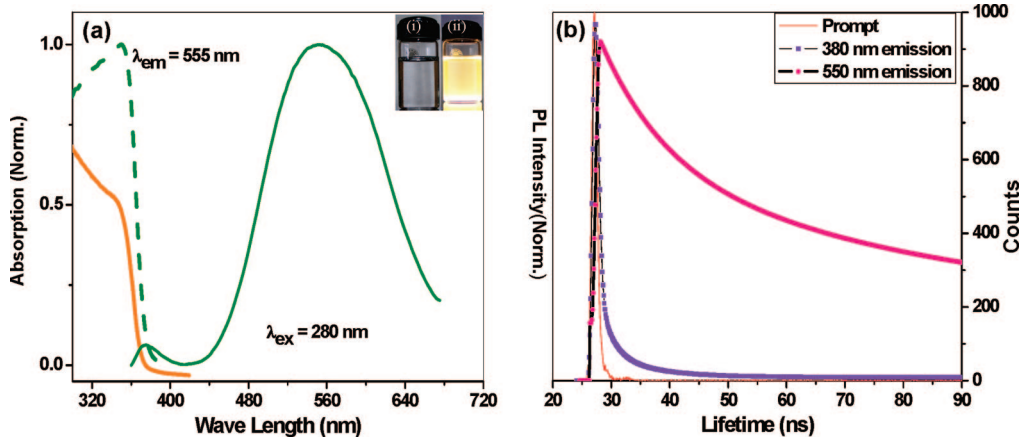

Figure 2. (a) Optical absorption and PL spectra of aqueous solutions of CMCD-capped ZnO:MgO. The excitation spectra obtained by monitoring the emission at 555 nm are shown by dashed lines. The inset shows digital photographs of the CMCD-capped ZnO:MgO aqueous solution illuminated by (i) normal laboratory light and (ii) UV radiation (312 nm). (b) Fluorescent lifetime decays of the aqueous CMCD ZnO:MgO solution monitored at 380 and 550 nm following excitation at 280 nm.

mole of ZnO:MgO, as determined by elemental analysis, was 4.17×10^{-3}. Assuming a uniform spherical particle size of 6 nm, this ratio would correspond to 20 CMCD cavities anchored to each of the ZnO:MgO nanocrystal particles.

As expected, the cyclodextrin-capped ZnO:MgO nanoparticles are very soluble in water. The solubility may be attributed to the exposed hydroxyl groups located on the wider rim of the cyclodextrin cavity. The proton NMR signals of the CMCD-capped ZnO:MgO nanocrystals dissolved in D_2O appear at similar positions as that of β-cyclodextrin but are considerably broadened because of immobilization of the cavities (see Supporting Information).

The UV−visible and photoluminescence (PL) spectra of aqueous solutions of the CMCD-capped ZnO:MgO nanocrystals are shown in Figure 2a. The optical absorption consists of a partially resolved band with a sharp onset corresponding to the excitonic transition of ZnO (Figure 2a). The observed optical band gap of 364 nm (3.4 eV) can be related to the dimension of the nanoparticles; the calculated ZnO particle size is 5.4 nm. The PL spectrum of the aqueous CMCD-capped ZnO:MgO on excitation at 280 nm exhibits an intense broad emission band in the visible centered at 555 nm and a much weaker, but sharper, emission at 375 nm. The visible emission is the dominant feature of the luminescence from the aqueous CMCD-capped ZnO:MgO, being about 40 times more intense than the UV emission and is stable for long periods of time (>30 days). The excitation spectrum obtained by monitoring the emission at 555 nm is similar to the absorption spectra. The PL spectra of the ZnO:MgO nanocrystals are characteristic of the ZnO core. This is not unexpected; the band gap of MgO is 7.8 eV compared to 3.4 eV of ZnO, and the valence band of MgO is offset by 1.48 eV below that of the ZnO valence band.[26] The ZnO:MgO core−shell structure would, therefore, correspond to a type I nanostructure wherein both the photogenerated electrons and holes are localized in the ZnO core.[27] The quantum yield of the visible emission of the CMCD-capped ZnO:MgO nanocrystals in water, estimated using quinine sulfate in 0.1 N H_2SO_4 as standard, is 7% (see Supporting Information). The fluorescence spectra of the CMCD-capped ZnO:MgO in water show no change in band position and quantum yields for pH values between 5 and 12 (see Supporting Information). The UV emission at 375 nm in the PL spectrum of the CMCD-capped ZnO:MgO results from the recombination of excitons, while the visible emission from recombination involving deep trap states arisies from oxygen vacancies and photogenerated charge carriers in shallow traps. This assignment is supported by lifetime measurements (Figure 2b). The average lifetime of the visible emission (36 ns) is much longer than that of the UV excitonic emission (2.5 ns); this is characteristic of emission involving deep trap states.[28] The mechanism of the visible light emission from aqueous solutions of the CMCD-capped ZnO:MgO nanocrystals appears to be similar to that recently proposed for the oleate-capped ZnO:MgO nanocrystals in nonpolar organic solvents.[23] The capping of ZnO:MgO nanocrystals with CMCD cavities provides a simple route for obtaining nanocrystals that are water-soluble and emit in the visible when exposed to UV.

The host−guest chemistry of the CMCD-capped ZnO:MgO nanocrystals was explored by investigating the inclusion of the organic dye, Nile Red, within the anchored cyclodextrin cavities; Nile Red is known to form a 1:1 inclusion complex with β-cyclodextrin. It was chosen as the guest molecule because its absorption spectrum has appreciable overlap with the emission spectrum of the ZnO:MgO nanocrystals while its absorption coefficient in the UV spectral range, 330−360 nm, where the ZnO:MgO nanocrystals are excited, is negligible (Figure 3). Nile Red has the added advantage for

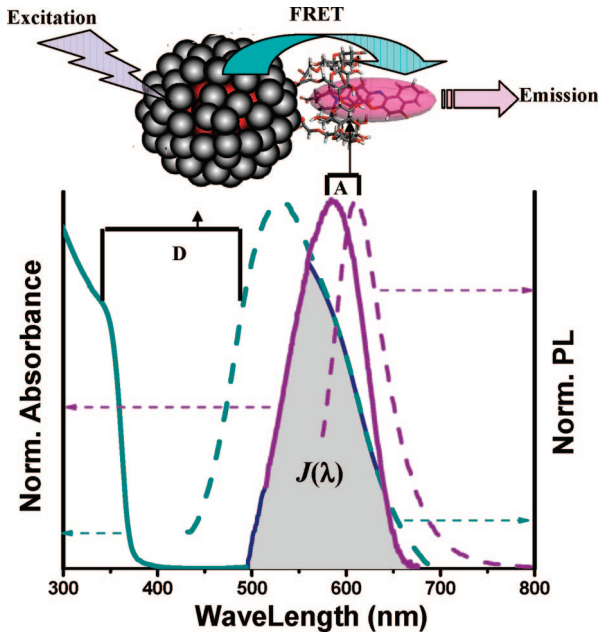

Figure 3. Schematic of the FRET process in CMCD ZnO:MgO−Nile Red assemblies (for clarity, only one anchored cyclodextrin cavity is shown). The normalized absorption (solid line) and photoluminescence (dashed line) spectra of the donor (D), CMCD-capped ZnO:MgO nanocrystals and the acceptor (A), Nile Red, in aqueous solutions are shown. The spectral overlap of the ZnO:MgO fluorescence (dotted, green) and the Nile Red absorption (solid, magenta) is shaded in gray.

the present study that it is poorly soluble in water. Fluorescence resonance energy transfer occurs when the electronic excitation energy of a donor chromophore is transferred to an acceptor molecule nearby *via* a dipole−dipole interaction between the donor−acceptor pair.[29] The FRET process is more efficient when there is an appreciable overlap between the emission spectrum of the donor and the absorption spectrum of the acceptor. Figure 3 shows that there is sufficient overlap between the PL bands of the ZnO:MgO nanocrystals and the absorption band of Nile Red. Effective Forster-type resonance energy transfer between the nanocrystals and the dye may, therefore, be anticipated if the donor−acceptor pair is not too far separated in the CMCD-capped ZnO:MgO−Nile Red assembly.

The PL spectra of aqueous solutions of the CMCD-capped ZnO:MgO nanocrystal donors with increasing amounts of added Nile Red acceptors are shown in Figure 4. The excitation wavelength, 356 nm, corresponded to the excitonic absorption band of the ZnO:MgO nanocrystal. The acceptor−donor ratios are expressed as the number of Nile Red molecules per anchored cyclodextrin cavity and also as the number of Nile Red molecules per ZnO:MgO nanocrystal. The latter assumes a uniform spherical particle size of 6 nm for the ZnO:MgO nanocrystals. With increasing acceptor−donor ratio, the visible emission of the ZnO:MgO nanocrystals between 510 and 580 nm is effectively quenched while there is an enhancement of the Nile Red emission at 640 nm. The spectra clearly indicate resonance energy transfer from the ZnO:MgO nanocrystals to the included Nile Red. It may be noted that the PL spectra in Figure 4 are the "as recorded" spectra. Because of the absence of any direct excitation of the Nile Red acceptor molecules at 356 nm, the spectra did not require any correction or deconvolution. Further evidence that the emission from Nile Red at 640 nm in the CMCD ZnO:MgO−Nile Red assembly arises from a resonance energy transfer process was established from the excitation spectra recorded by monitoring the Nile Red emission at 640 nm. The excitation spectra show a feature at 360 nm corresponding to the band gap excitation of the ZnO:MgO nanocrystal. The corresponding excitation spectra of Nile Red solubilized in water using β-cyclodextrin show no such feature. The presence of an iso-emissive point in Figure 4 is evidence that the inclusion of Nile Red may be described as a simple thermodynamic equilibrium between two species. This implies that the filling up of the anchored CMCD cavities by Nile Red molecules is an independent process. At higher concentrations of included Nile Red, when the ratio of included Nile Red to anchored cyclodextrin cavities exceeds 0.9, the ZnO:MgO−Nile Red assembly precipitates out of the aqueous solution. This occurs, presumably, because the surface of the nanocrystals when covered by included Nile Red molecules is no longer hydrophilic.

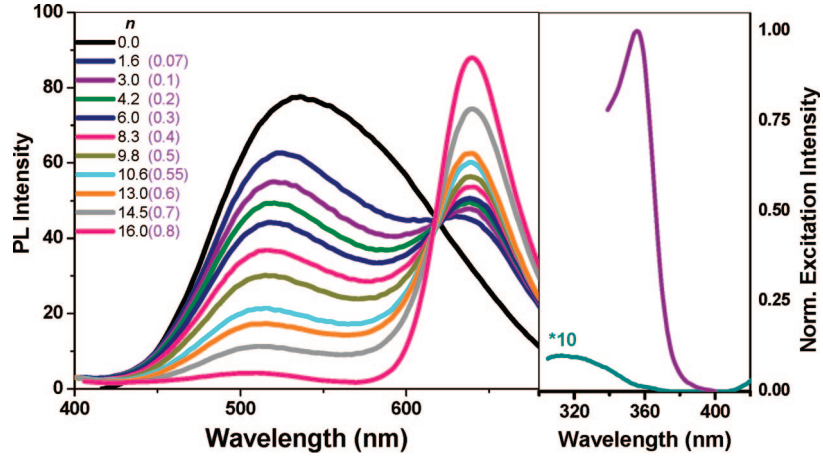

Figure 4. Evolution of the photoluminescence spectra of the CMCD−ZnO:MgO−Nile Red assembly with increasing Nile Red to ZnO:MgO ratio, *n*. The ratio of Nile Red molecules per anchored cyclodextrin cavity is shown in parentheses. The panel on the right shows the excitation spectra recorded by monitoring the Nile Red emission at 640 nm for a sample with $n = 10.6$. For comparison, the excitation spectra of the acceptor, Nile Red, solubilized in water using β-cyclodextrin, are also shown (green line).

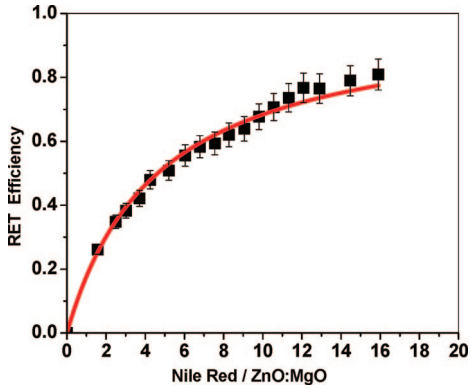

Figure 5. Variation of the resonance energy transfer (RET) efficiency with increasing Nile Red to ZnO:MgO ratio. The solid line is a fit to eq 4 for a donor–acceptor distance, *r*, of 4.3 nm.

The efficiency of the resonance energy transfer (RET) defined as $Q = (\mathbf{I}_{ZnO} - \mathbf{I}_{ZnO\text{-}NR})/\mathbf{I}_{ZnO}$, where $\boldsymbol{I}_{ZnO\text{-}NR}$ is the integrated fluorescence intensity of the ZnO:MgO donor in the CMCD−ZnO:MgO−Nile Red assembly and $\boldsymbol{I}_{ZnO}$ the integrated fluorescence intensity of an identical concentration of CMCD−ZnO:MgO in water in the absence of Nile Red has been plotted as a function of ratio of the number of acceptor Nile Red molecules to a ZnO:MgO nanocrystal donor in Figure 5. We have analyzed the variation in RET efficiencies with acceptor concentration assuming that the Forster mechanism is valid in the present situation.[4,29] In this formalism the RET efficiency is defined as

$$Q = \frac{k_{ZnO-NR}}{k_{ZnO-NR} + \tau_{ZnO}^{-1}} = \frac{R_0^{\,6}}{R_0^{\,6} + r^6} \qquad (1)$$

where τ_{ZnO} is the decay time of the ZnO:MgO donor in the absence of Nile Red and $k_{ZnO\text{-}NR}$ is the emission rate constant of the donor in an isolated CMCD ZnO:MgO−Nile Red pair separated by a distance *r*. R_0 is the critical distance, or Forster radius, at which transfer and spontaneous decay of the excited donor are equally probable, $k_{ZnO\text{-}NR} = \tau_{ZnO}^{-1}$. R_0 may be experimentally determined from the spectroscopic data and is given by

$$R_0 = \frac{9000(\ln 10)\kappa^2 \varphi_D^{\,0}}{128\pi^5 N_A \eta^4} J(\lambda) \qquad (2)$$

where κ^2 is an orientation factor and has a value of 2/3 for randomly oriented donor−acceptor dipoles, $\phi_D^{\,0}$ is the quantum yield of the donor in the absence of the acceptor, N_A is the Avogadro number, η is the refractive index of the medium, and $J(\lambda)$ is a quantitative measure of the donor−acceptor spectral overlap over all wavelengths (the shaded area in Figure 3) and is given by

$$J(\lambda) = \int_0^\infty I_D(\lambda)\varepsilon_A(\lambda)\lambda^4 d\lambda \qquad (3)$$

$I_D(\lambda)$ is the normalized fluorescence spectrum of the donor (CMCD-capped ZnO:MgO nanocrystals), and $\varepsilon_A(\lambda)$ is the absorption coefficient of the acceptor (Nile Red). For the CMCD ZnO:MgO−Nile Red assembly, the spectroscopically determined value of R_0 is 3.4 nm. For a donor interacting with multiple acceptors and if the energy transfer to each of the acceptors can be considered as independent events, then the efficiency of the transfer may be expressed as

$$Q = \frac{nR_0^{\,6}}{nR_0^{\,6} + r^6} \qquad (4)$$

where *n* is the number of acceptor molecules.[30] The value of *r*, the donor−acceptor distance in the CMCD ZnO:MgO−Nile Red assembly, was determined by fitting eq 4 to the experimentally observed variation of the transfer efficiency with acceptor concentration (Figure 5). The fit returned a value of 4.3 nm for *r*.

The resonance energy transfer in the CMCD-capped ZnO:MgO-Nile Red assembly has a number of unique features that distinguish it from similar studies using quantum dots (QDs). Unlike in the QDs, the energy transfer here is not from the excitonic emission but from emission originating from recombination of photogenerated electron and hole carriers that are trapped in surface states (shallow traps), with deep trap states arising from oxygen vacancies in the ZnO core. The visible emission in the ZnO:MgO nanocrystals has no corresponding "absorption" in the optical spectra since it arises from recombination of carriers that are generated by band gap excitation but subsequently trapped in shallow states that lie just below the conduction band or just above the valence band. It is for this reason that the excitation spectra (Figure 3) obtained by monitoring the Nile red emission in the CMCD-capped ZnO:MgO−Nile Red assembly show a feature at 360 nm corresponding to the band gap of the ZnO "core",

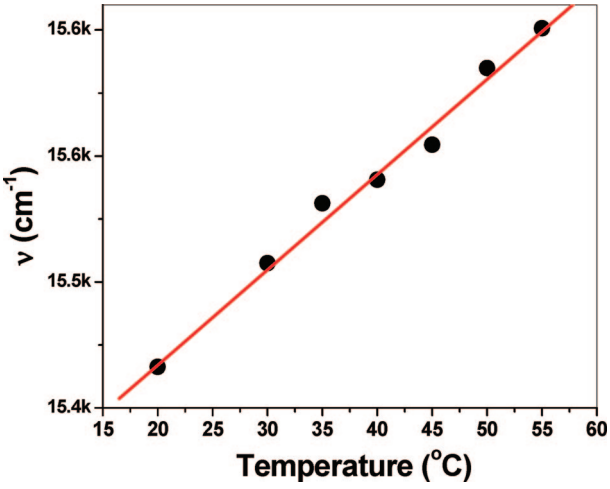

Figure 6. Thermochromic emission shifts for Nile Red included in the CMCD ZnO:MgO nanocrystals in aqueous solutions. The solid line is a linear fit with a thermochromic shift value of 3 cm^{-1}/K.

although the resonance energy transfer is from the visible emission at 530 nm of the ZnO:MgO donor. It may be seen that the excitation spectra of Nile Red in the CMCD ZnO:MgO−Nile Red assembly are identical to the excitation spectra of the visible emission of the CMCD ZnO:MgO donor (Figure 2). The second unique feature of the resonance energy transfer in the CMCD-capped ZnO:MgO−Nile Red assembly is that there is no direct linkage between donor and acceptor; they are held together by supramolecular interactions. The acceptor molecule, Nile Red, forms an inclusion complex with the cyclodextrin cavities that cap the ZnO:MgO nanocrystals. The interaction between Nile Red and the cyclodextrin cavity is dispersive in nature.

A characteristic feature of the fluorescence of Nile Red, in addition to its solvatochromic property, is thermochromism.[31] The emission shows a blue shift with increasing temperature. This property is retained by the Nile Red molecules in the cavities of the CMCD-capped ZnO:MgO nanocrystals. The position of the Nile Red emission, following resonance energy transfer, shifts to lower wavelengths with increasing temperature. Figure 5 shows how the emission energy of the included Nile Red varies with temperature in aqueous solutions. Over this temperature range, the variation is linear with a thermochromic shift value of 3 cm^{-1}/K. The reported thermochromic shift values for Nile Red in nonpolar solvents are in the range of 0.9 to 4 cm^{-1}/K.[31] The observed thermochromism of the CMCD ZnO:MgO−Nile Red assembly can in principle be used as a thermometer in aqueous solutions.

In conclusion, we have shown that capping of ZnO:MgO nanocrystals, prepared by a sequential synthetic procedure, with CMCD molecules provides a simple route for obtaining nanocrystals that are water-soluble and emit in the visible when exposed to UV. The emission is stable over a range of pH values and for extended periods of time. The integrity of the capping cyclodextrin cavities is preserved and available for host−guest chemistry. We have successfully demonstrated the inclusion of a hydrophobic dye, Nile Red, in the capping cyclodextrin cavities in aqueous solutions to form a noncovalent CMCD ZnO:MgO−Nile Red supramolecular assembly. We show that there is resonance energy transfer from the CMCD-capped ZnO:MgO nanocrystals to included Nile Red following band gap excitation of ZnO in the UV. A unique feature of the resonance energy transfer in the CMCD-capped ZnO:MgO−Nile Red assembly is that the energy transfer is from the visible trap state emission although the primary absorption is in the UV. The present work also highlights the versatility of using cyclodextrins as capping agents; its host−guest chemistry can impart additional functionality to the nanocrystal or QD. Here we have shown how the fluorescence properties of ZnO:MgO nanocrystals can be modified by inclusion of an organic dye within the cavities of the capping cyclodextrin.

METHODS

Materials. Zinc acetate dihydrate ($Zn(OAc)_2 \cdot 2H_2O$), magnesium acetate tetrahydrate ($Mg(OAc)_2 \cdot 4H_2O$), tetramethylammonium hydroxide ($N(CH_3)_4OH \cdot 4H_2O$, 97%), and Nile Red were procured from Sigma-Aldrich. Carboxymethyl β-cyclodextrin ($(C_{42}H_{70-n}O_{35}(CH_3COONa)_n$ (CMCD)), was received as a gift from Cerestar Co. (Hammond, IN, USA)). The average degree of substitution, *n*, was 3.8. All chemicals were used as received.

Synthesis of CMCD-Capped ZnO:MgO Core−Shell Nanocrystals. The CMCD-capped ZnO:MgO nanocrystals were synthesized by a two-step procedure. In the first step, ZnO:MgO nanocrystals were prepared by a sequential preparative procedure. In this procedure, the ZnO "core" was synthesized by dropwise addition of a stoichiometric amount of tetramethylammonium hydroxide (TMAH) dissolved in ethanol (0.55 M) to 30 mL of 0.1 M $Zn(OAc)_2 \cdot 2H_2O$ dissolved in DMSO followed by stirring for an hour. The MgO "shell" was subsequently formed by the simultaneous addition of 2 mL of 0.15 M $Mg(OAc)_2 \cdot 4H_2O$ in DMSO along with 1 mL of the TMAH base in ethanol to the above reaction mixture, followed by continuous stirring. The ZnO:MgO nanocrystals were precipitated by addition of ethyl acetate. Transmission electron microscopy (TEM) and X-ray diffraction measurements of the ZnO:MgO and that of ZnO nanocrystals with no Mg present precipitated from the reaction mixture after 15 days of aging showed that the average particle size of the ZnO:MgO (∼5 nm) nanocrystals is smaller than that of ZnO (∼12 nm) (see Supporting Information). The molar ratio of Mg to Zn, as determined by EDAX measurements, was ∼8%, while elemental mapping showed that individual particles had both Mg and Zn present (see Supporting Information). The ZnO:MgO nanocrystals were capped with CMCD by addition of 3 equiv of CMCD dissolved in DMSO to the as prepared ZnO:MgO solution dispersed in DMSO. The reaction mixture was stirred for 6 h at 50 °C, cooled to room temperature, and excess of acetonitrile added to obtain a white precipitate. The precipitate was then isolated by centrifuging and washed repeatedly with 3:1 water/DMSO solvent mixture and finally with 3:1 water/acetone. Stoichiometry was determined by elemental analysis (2.9 11% C, 1.19% H). The molar ratio of CMCD per mole of ZnO:MgO was 4.17×10^{-3}.

Physical Characterization. . Powder X-ray diffraction patterns were recorded on a Siemens D5005 X-ray diffractometer using Cu Kα radiation of $\bar{\lambda} = 1.54$ Å. Data were collected at a scan speed of 0.3 °/min with an increment of 0.1°. High-resolution transmission electron microscopy (HRTEM) images were collected on a Tecnai F30, FEI fitted with EDAX and elemental mapping attachments. Elemental analysis was done by ThermoFinnigan Flash EA 1112 CHNS analyzer. FT-IR spectra were recorded as KBr pellets on a Perkin-Elmer Spectrum One spectrometer operating at 4 cm^{-1} resolution. ^1H NMR spectra for CMCD and CMCD-capped ZnO:MgO nanocrystals dissolved in D_2O were recorded on a Bruker Avance 400 spectrometer. Absorption and photoluminescence spectra of CMCD-capped ZnO:MgO nanocrystals dissolved in water were recorded at room temperature on a Perkin-Elmer Lambda 35 UV−vis spectrometer and a Perkin-Elmer LS50 B luminescence spectrometer, respectively. Time-resolved fluorescence spectra were recorded in Fluoromax-4-TCSPC spectrofluorometer using a 280 nm Nano LED source for excitation. Quantum yields of the CMCD-capped ZnO:MgO nanocrystals were determined using quinine sulfate dye as reference (see Supporting Information).

FRET Measurements. For the FRET studies, the donor concentrations were kept constant while that of the acceptor varied. The solution of the donor was prepared by dissolving 400 mg of the CMCD-capped ZnO:MgO in 100 mL of milli-Q water. This corresponds to a concentration of anchored cyclodextrins of 0.019 M. Nile Red solutions of concentrations ranging from 0.5 to 1.5

mM in acetone were prepared. For the FRET measurements, 0.1 mL of the Nile Red solutions, of different concentrations, was added to 3 mL of the CMCD ZnO:MgO donor solution in a quartz cuvette, and the PL spectra were monitored continuously.

Acknowledgment. The carboxymethyl cyclodextrin was received as a gift from Cerestar Company (Hammond, IN).

Supporting Information Available: X-ray diffraction patterns and TEM images of 15 day aged ZnO:MgO and ZnO nanocrystals. EDAX spectrum of ZnO:MgO nanocrystals. Elemental mapping of Zn and Mg in ZnO:MgO nanocrystals. Infrared and Raman spectra and table of assignments of CMCD-capped ZnO:MgO nanocrystals. ^{1}H NMR of CMCD and CMCD-capped ZnO:MgO nanocrystals in D_2O. Fluorescence spectra of the water-soluble CMCD-capped ZnO:MgO nanocrystals recorded at different values of pH. Determination of the quantum yield for the visible emission from CMCD-capped ZnO:MgO nanocrystals in water. This material is available free of charge *via* the Internet at http://pubs.acs.org.

REFERENCES AND NOTES

1. Medintz, I. L.; Uyeda, H. T.; Goldman, E. R.; Mattoussi, H. Quantum Dot Bioconjugates for Imaging, Labelling and Sensing. *Nat. Mater.* **2005**, *4*, 435–446.
2. Alivisatos, A. P. Semiconductor Clusters, Nanocrystals, and Quantum Dots. *Science* **1996**, *271*, 933–937.
3. Bruchez, M., Jr.; Moronne, M.; Gin, P.; Weiss, S.; Alivisatos, A. P. Semiconductor Nanocrystals as Fluorescent Biological Labels. *Science* **1998**, *281*, 2013–2016.
4. Clapp, A. R.; Medintz, I. L.; Mattoussi, H. Forster Resonance Energy Transfer Investigations Using Quantum-Dot Fluorophores. *ChemPhysChem* **2006**, *7*, 47–57.
5. Wargnier, R.; Baranov, A. V.; Maslov, V. G.; Stsiapura, V.; Artemyev, M.; Pluot, M.; Sukhanova, A.; Nabiev, I. Energy Transfer in Aqueous Solutions of Oppositely Charged CdSe/ZnS Core/Shell Quantum Dots and in Quantum Dot−Nanogold Assemblies. *Nano Lett.* **2004**, *4*, 451–457.
6. Potapova, I.; Mruk, R.; Huebner, C.; Zentel, R.; Basche, T.; Mews, A. CdSe/ZnS Nanocrystals with Dye-Functionalized Polymer Ligands Containing Many Anchor Groups. *Angew. Chem., Int. Ed.* **2005**, *44*, 2437–2440.
7. Clapp, A. R.; Medintz, I. L.; Mauro, J. M.; Fisher, B. R.; Bawendi, M. G.; Mattoussi, H. Fluorescence Resonance Energy Transfer between Quantum Dot Donors and Dye-Labeled Protein Acceptors. *J. Am. Chem. Soc.* **2004**, *126*, 301–310.
8. Medintz, I. L.; Trammell, S. A.; Mattoussi, H.; Mauro, J. M. Reversible Modulation of Quantum Dot Photoluminescence Using a Protein-Bound Photochromic Fluorescence Resonance Energy Transfer Acceptor. *J. Am. Chem. Soc.* **2004**, *126*, 30–31.
9. Medintz, I. L.; Clapp, A. R.; Mattoussi, H.; Goldman, E. R.; Fisher, B.; Mauro, J. M. Self-Assembled Nanoscale Biosensors Based on Quantum Dot FRET Donors. *Nat. Mater.* **2003**, *2*, 630–638.
10. Goldman, E. R.; Medintz, I. L.; Whitley, J. L.; Hayhurst, A.; Clapp, A. R.; Uyeda, H. T.; Deschamps, J. R.; Lassman, M. E.; Mattoussi, H. A Hybrid Quantum Dot−Antibody Fragment Fluorescence Resonance Energy Transfer-Based TNT Sensor. *J. Am. Chem. Soc.* **2005**, *127*, 6744–6751.
11. Oh, E.; Hong, M. Y.; Lee, D.; Nam, S. H.; Yoon, H. C.; Kim, H. S. Inhibition Assay of Biomolecules Based on Fluorescence Resonance Energy Transfer (FRET) between Quantum Dots and Gold Nanoparticles. *J. Am. Chem. Soc.* **2005**, *127*, 3270–3071.
12. Zhou, D.; Piper, J. D.; Abell, C.; Klenerman, D.; Kang, D. J.; Ying, L. Fluorescence Resonance Energy Transfer between a Quantum Dot Donor and a Dye Acceptor Attached to DNA. *Chem Commun* **2005**, 4807–4809.
13. Wang, X. Y.; Ma, Q.; Li, B. Y.; Li, B.; Su, X. G.; Jin, Q. H. Studies on Fluorescence Resonance Energy Transfer between Dyes and Water-Soluble Quantum Dots. *Can. J. Anal. Sci. Spectrosc.* **2005**, *50*, 141–146.
14. Larson, D. R.; Zipfel, W. R.; Williams, R. M.; Clark, S. W.; Bruchez, M. P.; Wise, F. W.; Webb, W. W. Water-Soluble Quantum Dots for Multiphoton Fluorescence Imaging *In Vivo*. *Science* **2003**, *300*, 1434–1436.
15. Derfus, A. M.; Chan, W. C. W.; Bhatia, S. N. Probing the Cytotoxicity of Semiconductor Quantum Dots. *Nano Lett.* **2004**, *4*, 11–18.
16. Pradhan, N.; Battaglia, D. M.; Liu, Y.; Peng, X. Efficient, Stable, Small, and Water-Soluble Doped ZnSe Nanocrystal Emitters as Non-Cadmium Biomedical Labels. *Nano Lett.* **2007**, *7*, 312–317.
17. Dijken, A. V.; Meulenkamp, E. A.; Vanmaekelbergh, D.; Meijerink, A. Identification of the Transition Responsible For the Visible Emission in ZnO Using Quantum Size Effects. *J. Lumin.* **2000**, *90*, 123–128.
18. Batista, P. D.; Mulato, M. ZnO Extended-Gate Field-Effect Transistors as pH Sensors. *Appl. Phys. Lett.* **2005**, *87*, 143508–143510.
19. Wood, A.; Giersig, M.; Hilgendorff, M.; Vilas-Campos, A.; Liz-Marzan, L. M.; Mulvaney, P. Size Effects in ZnO: The Cluster to Quantum Dot Transition. *Aust J. Chem.* **2003**, *56*, 1051–1057.
20. Norberg, N. S.; Gamelin, D. R. Influence of Surface Modification on the Luminescence of Colloidal ZnO Nanocrystals. *J. Phys. Chem. B* **2005**, *109*, 20810–20816.
21. Bang, J.; Yang, H.; Holloway, P. H. Enhanced and Stable Green Emission of ZnO Nanoparticles by Surface Segregation of Mg. *Nanotechnology* **2006**, *17*, 973–978.
22. Studenikin, S. A.; Cocivera, M. Time-Resolved Luminescence and Photoconductivity of Polycrystalline ZnO Films. *J. Appl. Phys.* **2002**, *91*, 5060–5065.
23. Rakshit, S.; Vasudevan, S. Trap-State Dynamics in Visible-Light-Emitting ZnO:MgO Nanocrystals. *J. Phys. Chem. C* **2008**, *112*, 4531–4537.
24. Liu, J.; Mendoza, S.; Roman, E.; Lynn, M. J.; Xu, R.; Kaifer, A. E. Cyclodextrin-Modified Gold Nanospheres. Host−Guest Interactions at Work to Control Colloidal Properties. *J. Am. Chem. Soc.* **1999**, *121*, 4304–4305.
25. Peng, X. G.; Schlamp, M. C.; Kadavanich, A. V.; Alivisatos, P. A. Epitaxial Growth of Highly Luminescent CdSe/CdS Core/Shell Nanocrystals with Photostability and Electronic Accessibility. *J. Am. Chem. Soc.* **1997**, *119*, 7019–7029.
26. Lambrecht, W. R. L.; Limpijumnong, S.; Segall, B. Theoretical Studies of ZnO and Related $Mg_xZn_{1-x}O$ Alloy Band Structures. *MRS Int. J. Nitride Semicond. Res.* **1999**, *4SI*, G6.8.
27. Yu, K.; Zaman, B.; Ramanova, S.; Wang, D.-S.; Ripmeester, A. J. Sequential Synthesis of Type II Colloidal CdTe/CdSe Core−Shell Nanocrystals. *Small* **2005**, *1*, 332–338.
28. Brus, L. Electronic Wave Functions in Semiconductor Clusters: Experiment and Theory. *J. Phys. Chem.* **1986**, *90*, 2555–2560.
29. Lakowicz, J. R. *Principles of Fluorescence Spectroscopy*; Plenium Press: New York, 1983.
30. Clapp, A. R.; Medintz, I. L.; Uyeda, H. T.; Fisher, B. R.; Goldman, E. R.; Bawendi, M. G.; Mattoussi, H. Quantum Dot-Based Multiplexed Fluorescence Resonance Energy Transfer. *J. Am. Chem. Soc.* **2005**, *127*, 18212–18221.
31. Christina, M. G.; Williams, W. B.; Foresman, J. B. Further Solvatochromic, Thermochromic, and Theoretical Studies on Nile Red. *J. Fluoresc.* **1998**, *8*, 395–404.